

# Age of Information Analysis for Finite Blocklength Regime in Downlink Cellular Networks

Hyeonjun Sung<sup>1</sup>, Graduate Student Member, IEEE, Minsu Kim<sup>2</sup>, Graduate Student Member, IEEE, Sungjin Lee<sup>2</sup>, and Jemin Lee<sup>1</sup>, Member, IEEE

**Abstract**—With increase in real-time systems, users have come to demand information with low latency. However, as the blocklength becomes finite to reduce communication duration, the decoding error probability is newly considered. In this letter, we consider downlink cellular networks, where base stations (BSs) periodically transmit information with finite blocklength to a user. To analyze the freshness of information, we derive the average age of information (AoI) and the AoI violation probability in a closed-form using the upper bound of the average decoding error probability. Finally, we show that an optimal blocklength that minimizes the AoI exists.

**Index Terms**—Age of information, AoI violation probability, decoding error probability, finite blocklength.

## I. INTRODUCTION

AS THE number of Internet of Things (IoT) devices increases, the ultra-reliable low-latency communication (URLLC) that requires high reliability and low latency has been considered as the emerging application scenarios. Recently, some of the IoT devices (e.g., self-driving car) also require freshness data to make accurate decisions. Therefore, it is important to send information rapidly, but it is also important to maintain it fresh. Hence, some researchers have focused on the AoI, one of performance metrics for measuring the data freshness. The AoI is defined as the time elapsed since the generation of the most recently updated information [1].

In the studies of AoI, some works analyzed the freshness of information on the various queueing models [1], [2]. In [1], the authors analyzed the average AoI for a First-Come-First-Serve (FCFS) system in different three queueing models (i.e.,

M/M/1, M/D/1, and D/M/1). The peak AoI violation probability for D/Geo/1 queue and D/M/1 queue was analyzed in [2]. However, since the works in [1], [2] did not consider the retransmission scheme, there is a limitation that the AoI keeps increasing until the transmitter transmits new information.

Recently, some works in [3], [4] applied retransmission schemes to reduce the AoI. In [3], the authors presented AoI violation probability in a closed-form to analyze the error-tolerable sensing coverage. The optimal blocklength was presented to minimize the average AoI depending on the packet management schemes in [4]. However, the work in [3] only considered the user whose blocklength was assumed to be infinite, so that it is difficult to analyze the performance of URLLC users. Furthermore, one limitation in [4] is that they analyzed the average AoI, which cannot provide a result of the AoI distribution, in the absence of interfering nodes.

In this letter, we consider downlink cellular networks where BSs periodically transmit information received from an information generator (IG) via wired links to a user through wireless links. Within a sensing period, the transmission scheme is used with the limited maximum number of retransmissions to reduce the AoI. After deriving an upper bound of the average decoding error probability, we analyze the effect of the blocklength on the average AoI and the AoI violation probability. The main contributions of this letter can be summarized as follows: 1) we derive the average AoI and the AoI violation probability. 2) we then present an upper bound of the average decoding error probability to facilitate the AoI analysis. 3) we finally show the optimal blocklength that minimizes the AoI violation probability.

## II. SYSTEM MODEL

In this section, we introduce the network model and the communication model. We then characterize the AoI model.

### A. Network Model

As shown in Fig. 1, we consider a downlink cellular network where there exist multiple BSs, an IG, and users. The BSs are randomly distributed in a homogeneous poisson point process (HPPP)  $\Phi_B$  with density  $\lambda_B$ . The IG, which monitors its surrounding area (e.g., temperature and humidity), is located remotely, so it cannot directly transmit the information to users. Hence, the BSs transmit the information to users after getting it from the IG. It is assumed that it takes  $\mathcal{A}_0$  seconds for the information transfer from the IG to BSs.<sup>1</sup>

<sup>1</sup>Generally, IGs, which transfer its monitoring information periodically, are connected reliably to the networks such as over wired or wired-likely wireless channels. Hence, the time for information transfer can be assumed fixed.

Manuscript received November 2, 2021; revised December 13, 2021; accepted December 21, 2021. Date of publication December 30, 2021; date of current version April 11, 2022. This work was supported in part by the National Research Foundation of Korea (NRF) Grant funded by the Korea Government (MSIT) under Grant NRF-2018R1A5A1060031; in part by the Ministry of Science and ICT (MSIT), South Korea, under the Information Technology Research Center (ITRC) Support Program under Grant IITP-2020-0-01795 supervised by the Institute of Information & Communications Technology Planning & Evaluation (IITP); and in part by the National Research Foundation of Korea (NRF) Grant funded by the Korea Government (MSIP) under Grant 2020R1A2C2008878. The associate editor coordinating the review of this article and approving it for publication was J. Tang. (Corresponding author: Jemin Lee.)

Hyeonjun Sung is with the Technical Research Center, Innonet Company Ltd., Seoul 05836, South Korea (e-mail: hjsung@innonet.net).

Minsu Kim and Sungjin Lee are with the Department of Information and Communication Engineering, Daegu Gyeongbuk Institute of Science and Technology, Daegu 42988, South Korea (e-mail: ads5577@dgist.ac.kr; sungjin.lee@dgist.ac.kr).

Jemin Lee is with the Department of Electrical and Computer Engineering, Sungkyunkwan University, Suwon 16419, South Korea (e-mail: jemin.lee@skku.edu).

Digital Object Identifier 10.1109/LWC.2021.3139346

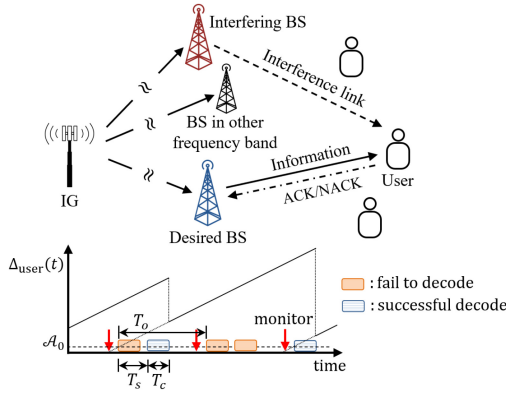


Fig. 1. System model where multiple BSs are randomly distributed in the network and they transmit the information received from an IG to a user.

In this network, BSs receive new information from the IG with period  $T_0$ . After the BSs receive the information, they transmit the information to a user during the transmission duration  $T_c = n_0 T_u$ . Here,  $n_0$  is the blocklength and  $T_u$  is the time allocated to the unit blocklength. However, since the user may not be able to decode the information, we consider the retransmission scheme. Specifically, if the user successfully decodes the information, the user sends an acknowledge (ACK) signal back to the BSs through error-free feedback link and the BS does not transmit the information to the user until new information arrives at the BS. On the other hand, if the user fails to decode the information, the user sends a negative acknowledgement (NACK) signal to BSs within  $T_s$ . When the BSs receive the NACK signal from the user, the BSs retransmit the information up to  $L$  times, and here, we have  $T_0 = LT_s$  where  $L$  is the maximum number of retransmissions and  $T_s$  is the retransmission period. If the transmitted information fails to be decoded at the user until new information arrives at BSs, the transmission is resumed using new information.

### B. Communication Model

The total available resource is divided into  $1/\mu$  sub-bands, therefore, interfering BSs are considered as the BSs that use the same resource. Here,  $\mu$  is a frequency reuse factor. The BSs, including the interfering BSs and a desired BS, are also randomly distributed in a HPPP  $\Phi_I$  with density  $\lambda_I = \mu\lambda_B$ . Under the considered network, when the typical user is associated with the nearest BS  $x_0 \in \Phi_B$ , the signal-to-interference ratio (SIR) at the user is given by<sup>2</sup>

$$\gamma_o = \frac{P_t h_o r_o^{-\alpha}}{\sum_{i \in \Phi_I \setminus \{x_0\}} P_t h_i r_i^{-\alpha}} = \frac{h_o r_o^{-\alpha}}{\sum_{i \in \Phi_I \setminus \{x_0\}} h_i r_i^{-\alpha}}, \quad (1)$$

where  $P_t$  is transmission power of the BS,  $\alpha$  is the path loss exponent,  $h_o$  is the channel fading gain between a user and an associated BS, and  $h_i$  is the channel fading gain between a user and the  $i$ -th interfering BS. We assume Rayleigh block fading channel, i.e.,  $h_o \sim \exp(1)$  and  $h_i \sim \exp(1)$ , which changes in an independent and identically distributed (i.i.d.) fashion in time [4]. In (1),  $r_o$  is the distance between a user and an associated BS and  $r_i$  is the distance between the typical

<sup>2</sup>In a downlink cellular network, since the number of interfering BSs is large, the interfering signal power is commonly much larger than noise power. Therefore, we consider the interference-limited environment.

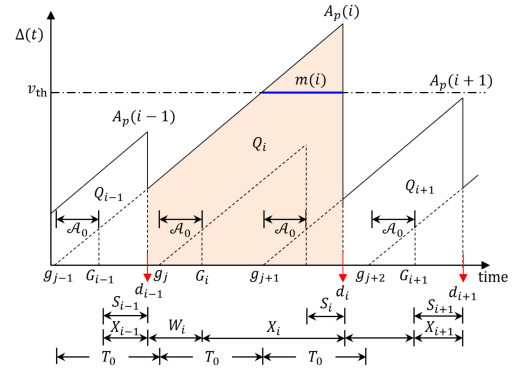


Fig. 2. A sample path of the AoI at the user. The index  $j$  is for the  $j$ -th information transmitted from the IG and the index  $i$  is for the  $i$ -th information arriving at the BS.

user and the  $i$ -th interfering BS. Using (1), the cumulative distribution function (CDF) of the SIR can be obtained as [5]

$$F_{\gamma_o}(x) = 1 - \mathbb{P}[\gamma_o \geq x] = \frac{\mu\rho(x, \alpha)}{1 + \mu\rho(x, \alpha)}, \quad (2)$$

where  $\rho(x, \alpha) = x^{2/\alpha} \int_{x^{-2/\alpha}}^{\infty} \frac{1}{1+u^{\alpha/2}} du$ .

In the finite blocklength regime, for given blocklength  $n_0$  and target rate  $R_t$ , the decoding error probability  $\varepsilon$  under normal approximation can be expressed as [6]

$$\varepsilon = Q\left(\frac{\log_2(1 + \gamma_o) - R_t}{\sqrt{V(\gamma_o)/n_0}}\right), \quad (3)$$

where  $Q(x) = \int_x^{\infty} \frac{1}{\sqrt{2\pi}} \exp(-\frac{t^2}{2}) dt$  is the Q-function,  $\gamma_o$  is given in (1),  $R_t = \frac{N}{n_0}$ ,  $N$  is the number of information bits, and  $V(\gamma_o)$  is the channel dispersion. In this network, since interfering BSs are considered, we cannot use the channel dispersion of the additive white Gaussian noise (AWGN) channel. This is because, when BSs use the non-Gaussian codebook, the user would be subject to non-Gaussian interference and the effective channel is no longer AWGN. Therefore, we employ the channel dispersion, where the BS uses the i.i.d. Gaussian codebook and the user employs the nearest-neighbor decoding, which is given by [7]

$$V(\gamma_o) = \frac{2\gamma_o}{1 + \gamma_o} (\log_2 e)^2. \quad (4)$$

### C. Age of Information

To measure how fresh information a user has at time  $t$ , we consider the AoI, defined as [1]

$$\Delta(t) = t - u(t), \quad (5)$$

where  $u(t)$  is the time stamp of the most recently decoded information. As shown in Fig. 2, when the user successfully decodes information, the AoI decreases to the age of the most recently decoded information, otherwise increases linearly.

In the AoI path, we define  $g_j$  as time that the  $j$ -th information is transmitted from the IG to BSs. We assume that the AoI at BSs is the same as  $\mathcal{A}_0$ . We then denote  $G_i$  as the latest time that information arrives at the BS after the  $(i-1)$ -th information successfully being decoded at the user.<sup>3</sup> After

<sup>3</sup>As transmitted information of the BS is not always successfully decoded at a user, we use different indexes  $i$  and  $j$  for  $G_i$  and  $g_j$ , respectively.

receiving information from the IG, the BSs start to transmit the information to the user. We denote  $d_i$  as time that the  $i$ -th information is successfully decoded at the user. Furthermore, we define the interval between  $G_i$  and  $d_i$  as  $X_i = d_i - G_i$ . Since the information is transmitted until it is successfully decoded,  $X_i$  follows the geometry distribution. The probability mass function (PMF) of  $X_i$  is given by

$$\mathbb{P}[X_i = (k-1)T_s + T_c] = (1-\bar{\varepsilon})\bar{\varepsilon}^{k-1}, \quad k = 1, 2, \dots, \quad (6)$$

where  $\bar{\varepsilon}$  is the average decoding error probability and  $k$  is the number of retransmissions.<sup>4</sup> In addition, for the  $i$ -th successful decoding, we denote  $S_i$  as the interval from the time received the most recent information at the BS (i.e.,  $g_{j+1} + \mathcal{A}_0$  in Fig. 2) to the time successfully decoded at the user (i.e.,  $d_i$  in Fig. 2). Due to the memoryless property, the PMF of  $S_i$  is not affected by the retransmissions, happened before the latest arrival of information at the BS. Hence,  $S_i = (\ell-1)T_s + T_c$  follows the truncated geometry distribution as  $\ell$ , the number of retransmissions in this case, cannot be greater than  $L$ . The PMF of  $S_i$  is then given by

$$\mathbb{P}[S_i = (\ell-1)T_s + T_c] = \frac{(1-\bar{\varepsilon})\bar{\varepsilon}^{\ell-1}}{1-\bar{\varepsilon}^L}, \quad \ell = 1, 2, \dots, L. \quad (7)$$

Furthermore,  $W_i = T_0 - S_{i-1}$  is the waiting time from the time  $d_{i-1}$  that  $(i-1)$ -th information is successfully decoded at the user to the time  $G_i$  that the  $i$ -th information arrives at the BS. We also define the peak AoI of the  $i$ -th information as  $A_p(i) = \mathcal{A}_0 + X_i + T_0$ .

The AoI analysis (e.g., the average AoI and the AoI violation probability) will be presented in Section IV after deriving the average decoding error probability.

### III. AVERAGE DECODING ERROR PROBABILITY

In this section, using (3), we analyze the average decoding error probability, given by

$$\bar{\varepsilon} = \int_0^\infty Q\left(\frac{\log_2(1+x) - R_t}{\sqrt{V(x)/n_0}}\right) f_{\gamma_o}(x) dx, \quad (8)$$

where  $f_{\gamma_o}(x)$  is obtained as  $\frac{dF_{\gamma_o}(x)}{dx} = f_{\gamma_o}(x)$ . Here,  $F_{\gamma_o}(x)$  is given by (2).

*Lemma 1:* The approximated average decoding error probability is presented as

$$\tilde{\varepsilon} = \sqrt{\frac{n_0}{4\pi(2^{2R_t} - 2R_t)}} \int_{x_1}^{x_2} \frac{\mu\rho(x, \alpha)}{1 + \mu\rho(x, \alpha)} dx, \quad (9)$$

where  $x_1 = 2^{R_t} - 1 - \sqrt{\frac{\pi(2^{2R_t} - 2R_t)}{n_0}}$  and  $x_2 = 2^{R_t} - 1 + \sqrt{\frac{\pi(2^{2R_t} - 2R_t)}{n_0}}$ .

*Proof:* Using the first-order Taylor approximation at  $x = 2^{R_t} - 1$ ,

$$Q\left(\frac{\log_2(1+x) - R_t}{\sqrt{V(x)/n_0}}\right)$$

<sup>4</sup>The average decoding error probability is obtained by averaging out the decoding error probability over channel distributions of main and interference links. The analysis of the average decoding error probability will be presented in Section III.

$$\approx \begin{cases} 1 & x < x_1 \\ \frac{1}{2} - \frac{\sqrt{n_0}}{\sqrt{4\pi(2^{2R_t} - 2R_t)}}(x - (2^{R_t} - 1)) & x_1 \leq x < x_2 \\ 0 & x \geq x_2 \end{cases}. \quad (10)$$

The average decoding error probability in (8) can be approximated as

$$\begin{aligned} \bar{\varepsilon} &\approx \tilde{\varepsilon} = \int_0^{x_1} f_{\gamma_o}(x) dx \\ &\quad + \int_{x_1}^{x_2} \left( \frac{1}{2} - \sqrt{\frac{n_0}{4\pi(2^{2R_t} - 2R_t)}} \{x - (2^{R_t} - 1)\} \right) f_{\gamma_o}(x) dx \\ &\stackrel{(a)}{=} \sqrt{\frac{n_0}{4\pi(2^{2R_t} - 2R_t)}} \int_{x_1}^{x_2} F_{\gamma_o}(x) dx, \end{aligned} \quad (11)$$

where (a) is from the partial integral. By substituting (2) into (11),  $\tilde{\varepsilon}$  is presented as (9). ■

Since  $\tilde{\varepsilon}$  in (9) does not have a closed-form expression, it is difficult to analyze the effect of network parameters on the average decoding error probability. Hence, we present the upper bound of it in a closed-form in the following corollary.

*Corollary 1:* The upper bound of the average decoding error probability  $\hat{\varepsilon}$  is given by

$$\begin{aligned} \hat{\varepsilon} &= 1 - \left( \frac{1}{2} + \sqrt{\frac{n_0(2^{R_t} - 1)}{4\pi 2^{R_t}}} \right) {}_2F_1\left(1, \frac{\alpha}{2}; \frac{2+\alpha}{2}; -\frac{2\mu\pi x_2^{2/\alpha}}{\alpha \sin(2\pi/\alpha)}\right) \\ &\quad + \left( -\frac{1}{2} + \sqrt{\frac{n_0(2^{R_t} - 1)}{4\pi 2^{R_t}}} \right) {}_2F_1\left(1, \frac{\alpha}{2}; \frac{2+\alpha}{2}; -\frac{2\mu\pi x_1^{2/\alpha}}{\alpha \sin(2\pi/\alpha)}\right), \end{aligned} \quad (12)$$

where  ${}_2F_1(a, b; c; d)$  is Gaussian hyper-geometric function.

*Proof:* Firstly, the CDF of the SIR  $\gamma_o$  is given by

$$F_{\gamma_o}(x) = \int_0^\infty F_{\gamma_o}(x|r) f_{r_o}(r) dr, \quad (13)$$

where  $f_{r_o}(r)$  is the probability distribution function (PDF) of the main link distance, given by [5]

$$f_{r_o}(r) = 2\pi\lambda_B \exp(-\pi\lambda_B r^2), \quad (14)$$

and  $F_{\gamma_o}(x|r)$  is the conditional CDF of  $\gamma_o$ , given by

$$\begin{aligned} F_{\gamma_o}(x|r) &= 1 \\ &\quad - \exp\left(-\pi\mu\lambda_B \int_r^\infty 2y(1 - \mathbb{E}_{h_i}[\exp(-xr^\alpha h_i y^{-\alpha})]) dy\right). \end{aligned} \quad (15)$$

In (15), by taking the integral range from 0 to  $\infty$  (instead of  $r$  to  $\infty$ ), we can obtain the upper bound of (15) as [8]

$$F_{\gamma_o}(x|r) \leq \hat{F}_{\gamma_o}(x|r) = 1 - \exp\left(-\pi\mu\lambda_B r^2 \frac{2\pi/\alpha}{\sin(2\pi/\alpha)} x^{\frac{2}{\alpha}}\right). \quad (16)$$

Using (13) and (16) in (11), we finally obtain the upper bound of  $\tilde{\varepsilon}$ , i.e.,  $\hat{\varepsilon} \geq \tilde{\varepsilon}$ , where  $\hat{\varepsilon}$  is given by

$$\begin{aligned} \hat{\varepsilon} &\stackrel{(a)}{=} \pi\lambda_B \sqrt{\frac{n_0}{4\pi(2^{2R_t} - 2R_t)}} \int_{x_1}^{x_2} \int_0^\infty [\exp(-\pi\lambda_B z) \\ &\quad - \exp\left\{-\pi\lambda_B z \left(\frac{2\pi\mu}{\alpha \sin(2\pi/\alpha)} x^{\frac{2}{\alpha}} + 1\right)\right\}] dz dx \\ &= \sqrt{\frac{n_0}{4\pi(2^{2R_t} - 2R_t)}} \int_{x_1}^{x_2} \left(1 - \frac{1}{\frac{2\pi\mu}{\alpha \sin(2\pi/\alpha)} x^{\frac{2}{\alpha}} + 1}\right) dx, \end{aligned} \quad (17)$$

where (a) is obtained by substitution from  $r^2$  to  $z$ . Using the following result [9, eq. (3.194)]

$$\int_0^u \frac{x^{\varphi-1}}{(1+\beta x)^\nu} dx = \frac{u^\varphi}{\varphi} {}_2F_1(\nu, \varphi; 1+\varphi; -\beta u), \quad (18)$$

with  $\varphi = \frac{\alpha}{2}$ ,  $\beta = \frac{2\pi\mu}{\alpha \sin(2\pi/\alpha)}$ ,  $u = x_1^{2/\alpha}$  (or  $u = x_2^{2/\alpha}$ ), and  $\nu = 1$ ,  $\hat{\varepsilon}$  can be presented in a closed-form as (12). ■

From Corollary 1, we can know the effect of the blocklength  $n_0$  on the upper bound of the average decoding error probability  $\hat{\varepsilon}$ . Furthermore, using (12), we can easily obtain the effect of  $n_0$  on the average AoI and the AoI violation probability.

#### IV. AGE OF INFORMATION ANALYSIS

In this section, we analyze the average AoI and the AoI violation probability.

##### A. Average AoI Analysis

In this subsection, we derive the average AoI, defined as [1]

$$\bar{\Delta} = \lim_{T \rightarrow \infty} \frac{1}{T} \int_0^T \Delta(t) dt \approx \frac{\mathbb{E}[Q_i]}{\mathbb{E}[d_i - d_{i-1}]}, \quad (19)$$

where  $Q_i = \frac{1}{2}(2\mathcal{A}_0 + S_{i-1} + X_i + T_0)(X_i + W_i)$  is the AoI area between  $(i-1)$ -th and  $i$ -th successful updates. From (19), we provide the average AoI in the following Lemma.

*Lemma 2:* The average AoI can be obtained as

$$\bar{\Delta} = \mathcal{A}_0 + \frac{(L-2)T_s}{2} + \frac{T_s}{1-\bar{\varepsilon}} + T_c. \quad (20)$$

*Proof:* In (19),  $\mathbb{E}[Q_i]$  and  $\mathbb{E}[d_i - d_{i-1}]$  is represented as

$$\mathbb{E}[Q_i] = \mathbb{E}\left[\frac{1}{2}(2\mathcal{A}_0 + S_{i-1} + X_i + T_0)(X_i + W_i)\right] \quad (21)$$

$$\stackrel{(a)}{=} \frac{1}{2}\mathbb{E}[(T_0 + X_i)^2] - \frac{1}{2}\mathbb{E}[S_i^2] + \mathcal{A}_0 T_0 - \mathcal{A}_0 \mathbb{E}[S_i] + \mathcal{A}_0 \mathbb{E}[X_i],$$

$$\mathbb{E}[d_i - d_{i-1}] = \mathbb{E}[W_i + X_i] \stackrel{(a)}{=} T_0 - \mathbb{E}[S_i] + \mathbb{E}[X_i], \quad (22)$$

where (a) holds as  $S_i$  and  $S_{i-1}$  are identically distributed.

Firstly, from (6), we obtain  $\mathbb{E}[X_i]$  and  $\mathbb{E}[X_i^2]$  as

$$\mathbb{E}[X_i] = \sum_{\ell=1}^{\infty} \{(\ell-1)T_s + T_c\}(1-\bar{\varepsilon})\bar{\varepsilon}^{\ell-1} = \frac{\bar{\varepsilon}}{1-\bar{\varepsilon}} T_s + T_c, \quad (23)$$

$$\begin{aligned} \mathbb{E}[X_i^2] &= \sum_{\ell=1}^{\infty} \{(\ell-1)T_s + T_c\}^2 (1-\bar{\varepsilon})\bar{\varepsilon}^{\ell-1} \\ &= \frac{2T_s^2}{(1-\bar{\varepsilon})^2} - \frac{(3T_s - 2T_c)T_s}{1-\bar{\varepsilon}} + (T_s - T_c)^2. \end{aligned} \quad (24)$$

From (7),  $\mathbb{E}[S_i]$  and  $\mathbb{E}[S_i^2]$  are also obtained as

$$\begin{aligned} \mathbb{E}[S_i] &= \sum_{\ell=1}^L \{(\ell-1)T_s + T_c\} \frac{(1-\bar{\varepsilon})\bar{\varepsilon}^{\ell-1}}{1-\bar{\varepsilon}^L} \\ &= \frac{T_s \{1 - \bar{\varepsilon}^L(1 + (1-\bar{\varepsilon})L)\}}{(1-\bar{\varepsilon})(1-\bar{\varepsilon}^L)} - T_s + T_c, \end{aligned} \quad (25)$$

$$\begin{aligned} \mathbb{E}[S_i^2] &= \sum_{\ell=1}^L \{(\ell-1)T_s + T_c\}^2 \frac{(1-\bar{\varepsilon})\bar{\varepsilon}^{\ell-1}}{1-\bar{\varepsilon}^L} \\ &\stackrel{(a)}{=} (T_s - T_c)^2 + \frac{T_s}{(1-\bar{\varepsilon})(1-\bar{\varepsilon}^L)} \left[ \frac{T_s}{(1-\bar{\varepsilon})} \left\{ -L^2 \bar{\varepsilon}^{L+2} \right. \right. \\ &\quad \left. \left. + (2L^2 + 2L - 1)\bar{\varepsilon}^{L+1} - (L+1)^2 \bar{\varepsilon}^L - (1-\bar{\varepsilon}) + 2 \right\} \right. \\ &\quad \left. - 2(T_s - T_c) \left\{ 1 - \bar{\varepsilon}^L(1 + (1-\bar{\varepsilon})L) \right\} \right]. \end{aligned} \quad (26)$$

where (a) is obtained from [9, eq. (0.114)]. By using (23), (24) and (26) in (21), and using (23) and (25) in (22), we obtain  $\mathbb{E}[Q_i]$  and  $\mathbb{E}[d_i - d_{i-1}]$  as

$$\mathbb{E}[Q_i] = \frac{LT_s}{1-\bar{\varepsilon}^L} \left( \frac{T_s}{1-\bar{\varepsilon}} + \frac{(L-2)T_s}{2} + T_c + \mathcal{A}_0 \right), \quad (27)$$

$$\mathbb{E}[d_i - d_{i-1}] = \frac{LT_s}{1-\bar{\varepsilon}^L}. \quad (28)$$

By using (27) and (28) in (19), we finally obtain (20). ■

From Lemma 2, we can know that the average AoI  $\bar{\Delta}$  increases as the maximum number of retransmissions  $L$  and the transmission duration  $T_c$  increase. Furthermore, since  $\bar{\Delta}$  increases with  $\bar{\varepsilon}$ , i.e.,  $\frac{\partial \bar{\Delta}}{\partial \bar{\varepsilon}} \geq 0$ , we can say that  $\bar{\Delta}$  with  $\hat{\varepsilon}$  is the upper bound of  $\bar{\Delta}$ . We now define  $\bar{\Delta}$  with  $\hat{\varepsilon}$  as  $\hat{\Delta}$ , which is the upper bound of the average AoI.

##### B. AoI Violation Probability Analysis

For given the AoI violation threshold  $v_{th}$ , the AoI violation probability is defined as [10]

$$p_v(v_{th}) = \mathbb{P}[\Delta(t) > v_{th}] = \frac{\mathbb{E}[m(i)]}{\mathbb{E}[d_i - d_{i-1}]}, \quad (29)$$

where  $m(i)$  is the time duration of  $i$ -th information, for which the AoI is larger than the AoI violation threshold, defined as

$$m(i) = \begin{cases} 0 & \text{if } A_p(i) < v_{th} \\ A_p(i) - v_{th} & \text{if } \mathcal{A}_0 + S_{i-1} < v_{th} \leq A_p(i) \\ d_i - d_{i-1} & \text{if } v_{th} \leq \mathcal{A}_0 + S_{i-1}, \end{cases} \quad (30)$$

According to the value of  $v_{th}$ , the expectation of  $m(i)$  in (30) can be obtained in a closed-form [3]. For  $\mathcal{A}_0 < v_{th} < \mathcal{A}_0 + T_0$ ,  $\mathbb{E}[m(i)]$  is given by

$$\begin{aligned} \mathbb{E}[m(i)] &= \frac{(1-\bar{\varepsilon}^b)\{T_s + (1-\bar{\varepsilon})(\mathcal{A}_0 - T_s - v_{th} + T_c)\}}{(1-\bar{\varepsilon})(1-\bar{\varepsilon}^L)} \\ &\quad + \frac{T_s(L - b\bar{\varepsilon}^b)}{1-\bar{\varepsilon}^L}, \end{aligned} \quad (31)$$

where  $b = \lfloor \frac{v_{th} - \mathcal{A}_0 - T_c}{T_s} \rfloor + 1$ . For  $v_{th} \geq \mathcal{A}_0 + T_0$ ,  $\mathbb{E}[m(i)]$  is given by

$$\mathbb{E}[m(i)] = \left\{ T_s \left( \frac{1}{1-\bar{\varepsilon}} + b - 1 \right) + T_c - v_{th} + \mathcal{A}_0 \right\} \bar{\varepsilon}^{b-L}. \quad (32)$$

Note that due to the space limitation, we omit the analysis of  $\mathbb{E}[m(i)]$ . The detail of derivation of  $\mathbb{E}[m(i)]$  can be presented in [3]. By substituting (28), (31), and (32) into (29), we can obtain the AoI violation probability as

1) Case 1 ( $\mathcal{A}_0 < v_{th} < \mathcal{A}_0 + T_0$ ):

$$\begin{aligned} p_v(v_{th}) &= \frac{(1-\bar{\varepsilon}^b)\{T_s + (1-\bar{\varepsilon})(\mathcal{A}_0 - T_s - v_{th} + T_c)\}}{(1-\bar{\varepsilon})LT_s} \\ &\quad + \frac{L - b\bar{\varepsilon}^b}{L}, \end{aligned} \quad (33)$$

2) Case 2 ( $v_{th} \geq \mathcal{A}_0 + T_0$ ):

$$\begin{aligned} p_v(v_{th}) &= \frac{(\bar{\varepsilon}^{b-L} - \bar{\varepsilon}^b)\{(1-\bar{\varepsilon})(\mathcal{A}_0 + T_c - v_{th}) + T_s\}}{(1-\bar{\varepsilon})LT_s} \\ &\quad + \frac{(\bar{\varepsilon}^{b-L} - \bar{\varepsilon}^b)(b-1)}{L}. \end{aligned} \quad (34)$$

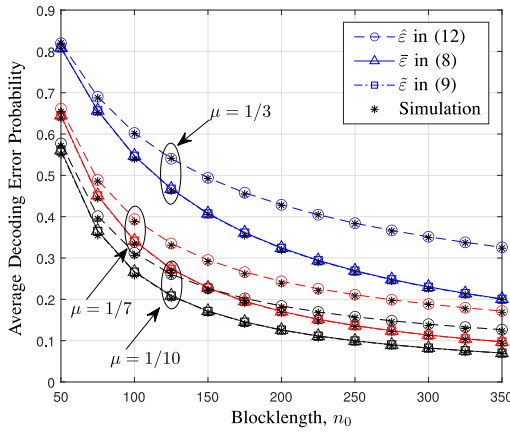


Fig. 3. Average decoding error probabilities as a function of  $n_0$  for different values of  $\mu$ .

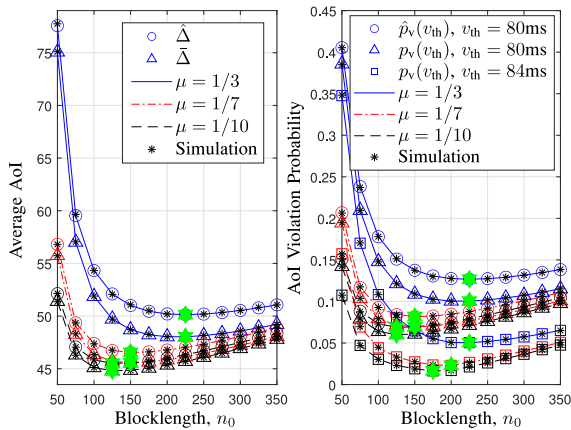


Fig. 4. Average AoI and AoI violation probability as a function of  $n_0$  for different values of  $\mu$  and  $v_{th}$ . The optimal blocklengths that minimize the average AoI and the AoI violation probability are marked by hexagrams.

**Remark 1:** The AoI violation probability  $p_v(v_{th})$  increases with the average decoding error probability  $\bar{\epsilon}$ , i.e.,  $\frac{\partial p_v(v_{th})}{\partial \bar{\epsilon}} \geq 0$  [3]. From this result, since  $\hat{\epsilon}$  is always larger than the  $\bar{\epsilon}$ , we can see that  $p_v(v_{th})$  with  $\hat{\epsilon}$  is the upper bound of  $p_v(v_{th})$ .

From Remark 1, we define  $p_v(v_{th})$  with  $\hat{\epsilon}$  as  $\hat{p}_v(v_{th})$ , which is the upper bound of the AoI violation probability.

## V. NUMERICAL RESULT

In this section, we analyze the effect of the blocklength on the average decoding error probability and the AoI analysis. Unless otherwise specified, the values of simulation parameters are  $N = 256$  bits,  $L = 10$ ,  $\mathcal{A}_0 = 0.2\text{ms}$ ,  $T_u = 0.02\text{ms}$ ,  $T_s = 8\text{ms}$ ,  $\alpha = 3.5$ , and  $\lambda_B = 10^{-6}$  [nodes/ $m^2$ ].

From Figure 3, we can see that the average decoding error probability decreases as the blocklength  $n_0$  increases. This is because as  $n_0$  increases, the effect of the channel dispersion on the average decoding error probability decreases. We can also see that  $\bar{\epsilon}$  in (8) and  $\hat{\epsilon}$  in (9) are almost the same. Furthermore, we can know that even though there is a gap between upper bound of the average decoding error probability  $\hat{\epsilon}$  and the average decoding error probability  $\bar{\epsilon}$ ,  $\hat{\epsilon}$  has a similar trend to  $\bar{\epsilon}$ . In addition, we can see that the analysis results closely match with the simulation results.

From Figure 4, we can see that the average AoI and the AoI violation probability first decrease up to a certain value of the

blocklength  $n_0$ , and then increase. This is because for small  $n_0$ , the decrease in the average decoding error probability is larger than the increase in the transmission duration  $T_c$ . On the other hand, for large  $n_0$ , as  $n_0$  increases, the increase in  $T_c$  is much greater than the decrease in the average decoding error probability. We can also see that original functions (i.e.,  $\hat{\Delta}$  and  $p_v(v_{th})$ ) and upper bounds (i.e.,  $\hat{\Delta}$  and  $\hat{p}_v(v_{th})$ ) have a similar trend and optimal blocklengths of original functions and upper bounds that minimize the average AoI and the AoI violation probability are the same. Hence, the optimal blocklength of the upper bound can be used to find the optimal blocklength of the original function. In addition, the optimal value of  $n_0$  increases as the frequency reuse factor  $\mu$  increases or the AoI violation threshold  $v_{th}$  increases. From this, we can know that as the effect of the interfering node increases or the AoI violation threshold increases, the larger blocklength needs to be used to decrease the average decoding error probability even though the transmission duration increases.

## VI. CONCLUSION

In this letter, we consider a downlink cellular network where a user cannot receive the information directly from an IG. Under such a network, when the maximum number of retransmissions is limited within a sensing period, we present the average AoI and the AoI violation probability. We then present an upper bound of the average decoding error probability to obtain the closed expression of the AoI and the AoI violation probability. In numerical results, we provide that even if there is a difference between the average decoding error probability and its upper bound, the trends are the same. Furthermore, we show that as the frequency reuse factor increases, the optimal blocklength increases to reduce the decoding error probability even though the transmission duration increases.

## REFERENCES

- [1] S. Kaul, R. Yates, and M. Gruteser, "Real-time status: How often should one update?" in *Proc. IEEE Conf. Comput. Commun.*, Orlando, FL, USA, Mar. 2012, pp. 1–5.
- [2] J. Seo and J. Choi, "On the outage probability of peak age-of-information for D/G/1 queuing systems," *IEEE Commun. Lett.*, vol. 23, no. 6, pp. 1021–1024, Jun. 2019.
- [3] J. Kim, M. Kim, and J. Lee, "Securing fresh data in wireless monitoring networks: Age-of-information sensitive coverage perspective," 2021, *arXiv:2103.07149*.
- [4] B. Yu, Y. Cai, D. Wu, and Z. Xiang, "Average age of information in short packet based machine type communication," *IEEE Trans. Veh. Technol.*, vol. 69, no. 9, pp. 10306–10319, Sep. 2020.
- [5] J. G. Andrews, F. Baccelli, and B. K. Ganti, "A tractable approach to coverage and rate in cellular networks," *IEEE Trans. Commun.*, vol. 59, no. 11, pp. 3122–3134, Nov. 2011.
- [6] Y. Polyanskiy, H. V. Poor, and S. Verdú, "Channel coding rate in the finite blocklength regime," *IEEE Trans. Inf. Theory*, vol. 56, no. 5, pp. 2307–2359, May 2010.
- [7] J. Scarlett, V. Y. F. Tan, and G. Durisi, "The dispersion of nearest-neighbor decoding for additive non-Gaussian channels," *IEEE Trans. Inf. Theory*, vol. 63, no. 1, pp. 81–92, Jan. 2017.
- [8] S. Weber, J. G. Andrews, and N. Jindal, "An overview of the transmission capacity of wireless networks," *IEEE Trans. Commun.*, vol. 58, no. 12, pp. 3593–3604, Dec. 2010.
- [9] I. S. Gradshteyn and I. M. Ryzhik, *Table of Integrals, Series, and Products*, 7th ed. San Diego, CA, USA: Academic, 2007.
- [10] J. P. Champati, H. Al-Zubaidy, and J. Gross, "On the distribution of AoI for the GI/GI/1/1 and GI/GI/1/2\* systems: Exact expressions and bounds," in *Proc. IEEE Conf. Comput. Commun.*, Paris, France, May 2019, pp. 37–45.